Phytic Acid-based NP Fire Retardant and its Effect on Combustion Property of Poplar Wood

Shenglei Qin,[1†] Yangguang Liu,[1†] Xin Shi, Xiaoshuang Shen, Demiao Chu,* and Shengquan Liu *

To enhance the synergistic effect of phosphorus (P) and nitrogen (N) on flame retardant property, four different phytic acid-based NP flame retardants (FR-PAN) were manufactured using phytic acid and urea with various molar ratios, ranging from 1:3 to 1:12. The FR-PAN water solution was used to impregnate poplar wood under vacuum condition, and the thermal degradation performance of the FR-PAN treated wood were investigated. Compared to untreated wood, the PAN-6 (molar ratio is 1:6) group showed a reduction of 57.1% in total heat release and 80.0% in total smoke release. In the combustion, due to the introduction of P and N, FR-PAN generates O=P/C-O/C-P/C-N bonds, forming highly graphitized char residues, which effectively isolate the entry of oxygen and heat and play a good protective role in the condensed phase. Morphological and chemical analysis of the residual char layer revealed that the introduction of P and N elements formed a more stable hybrid structure, significantly improving the thermal stability of the char layer. Among them, the PAN-6 group exhibited the highest char layer stability, indicating optimal synergistic effects of nitrogen and phosphorus under these conditions.

Contact information: School of Forestry & Landscape Architecture, Anhui Agricultural University, Hefei 230036, China; [1†]: Authors are co-first authors;
*Corresponding authors: demiaochu@ahau.edu.cn; liusq@ahau.edu.cn

INTRODUCTION

As a natural and environmentally friendly biopolymer group, wood has extensive use in the construction industry, and the demand for wood is rapidly increasing in many industrial sectors (Chen *et al.* 2020; Tang *et al.* 2021). The inherent flammability of wood (Chen *et al.* 2019; Zheng *et al.* 2022) poses a significant risk to human life and restricts the application of wood products. To improve the fire safety of wood, various flame retardants, such as phosphorus (Xia *et al.* 2014; Li *et al.* 2019; Song *et al.* 2020), nitrogen (Attia *et al.* 2016; Yu *et al.* 2020; Zhang *et al.* 2020), boron (Yang *et al.* 2016; Cheng *et al.* 2020), and silicon-based compounds (Zhu *et al.* 2019; Zhang *et al.* 2021), have been introduced through coating or impregnation techniques (Fan *et al.* 2022). Among these, intumescent flame retardants have gained popularity due to their low smoke production, low toxicity, excellent flame retardancy (Liu *et al.* 2011; Lin *et al.* 2021), and cost-effectiveness during combustion. Traditional intumescent flame retardants typically consist of ammonium polyphosphate as the dehydrating agent, pentaerythritol as the char-forming agent, and melamine as the blowing agent (Grancaric *et al.* 2015; Liu *et al.* 2020). Compared with non-intumescent flame retardant coatings, intumescent flame retardants are increasingly

preferred due to their superior performance characteristics and low cost.

There have been numerous studies on nitrogen and phosphorus-based flame retardants. To effectively reduce the release of smoke particles, the presence of a thick char layer as a physical barrier is essential (Tong *et al.* 2023). This protective char layer not only hinders rapid pyrolysis of the underlying wood and reduces the formation of gaseous products (Liu *et al.* 2023), but it also restricts the transfer of smoke precursors or particles (Giraud *et al.* 2013). Many compounds are used in combination with phytic acid to enhance smoke suppression efficiency by improving the stability of char residues (Zhang *et al.* 2022). Li *et al.* (2021) incorporated hydrolyzed collagen (HC) and glycerol (GL) with phytic acid in the wood cell cavity to create an expansive flame-retardant system, resulting in a significant increase in the residue char of the flame-retardant wood. Furthermore, the introduction of heteroatoms to form cross-linked structures in residues char has improved the flame retardancy and smoke suppression properties of wood composites (Wang *et al.* 2021). Yang *et al.* (2013) developed a phytic acid (PA)-silica hybrid system. The phytate-silica hybrid sol (PS) facilitated the generation of coherent and cross-linked residues char during combustion. The results showed that the total heat release and total smoke release of the PS/wood composite were 49.8% and 81.2%, which were lower than those of untreated wood, respectively. The flame retardant efficiency of the aforementioned system is relatively low, however, requiring a high flame retardant load (up to 51%) to meet the desired flame retardant performance, which significantly affects the practical application of phytic acid-based flame retardants (Dhineshbabu *et al.* 2014). The limited enhancement effect of the flame retardant system on the stability of residues char is the main reason behind its poor flame retardant effect.

Most studies have shown that nitrogen and phosphorus synergies exist in expansive flame retardants, but the effect of the ratio of the two on the synergies has not been considered. Only a few studies have shown that the different ratio of char source and acid source in intumescent flame retardants have different effects on flame retardancy (Wang *et al.* 2022). More importantly, to obtain good flame retardant properties, it is usually preferred to incorporate strong acid flame retardants into the wood matrix, but the penetration of strong acid phosphorous flame retardants into the wood structure may damage the complete structure of the wood (Cheng *et al.* 2015). It may also affect the mechanical properties of the wood. This inspired the authors to change the ratio of acid source (P) and gas source (N), and dip N and P co-flame retardant into wood cells to enhance N and P co-action.

This study explored the effect of the additional amount of air source and acid source on the flame retardant performance of intumescent flame retardants. The experiments incorporated bio-based organic acid PA as dehydrating agent, six char rings on phytic acid groups as a char forming agent, and urea (GL) as blowing agent. This combination was used to prepare a water-soluble nitrogen and phosphorus flame retardant through the complex reaction. These flame retardants were dissolved in water. Negative pressure vacuum impregnation was used to prepare environmentally friendly flame retardant wood. The smoke suppression, thermal stability, and combustion behavior of environmentally friendly flame retardant wood were analyzed, and the flame retardant mechanism of condensed phase and gas phase was explored. This environmentally friendly flame retardant system will provide a new way for sustainable and simple flame retardant treatment of wood.

EXPERIMENTAL

Materials

Poplar wood were collected from Fuyang Forest Farm, Anhui Province (Variety: poplar cultivar 'Jianghuai No.1', age 7 years, air-dried wood；the 3.3 to 5.3 m section was selected).

Phytic acid (PA, $C_6H_{18}O_{24}P_6$, 50% aqueous solution), ethanol (C_2H_6O, 99.7%), and urea (CH_4N_2H, 99%) were purchased from McLean Company (Shanghai, China).

Preparation of FR-PAN and Modified Wood

Preparation of flame retardants

A certain amount of 50% phytic acid solution was heated while stirring magnetically in a 250 mL three-neck flask at a speed of 300 r/min, using an oil bath at 120 °C. A reflux device was installed to achieve uniform heat distribution and prevent the reagent from drying. When the temperature of the system reached 60 °C, 60.06 g of urea was added (molar ratio of PA to urea =1:3, 1:6, 1:10, 1:12). It was reacted at 120 °C for 5 h to obtain a yellow oily transparent liquid. Then it was cooled to room temperature and frozen at -80 °C for 24 h. It was freeze-dried at -80 °C for 24 h to obtain white flame-retardant-PAN (FR-PAN-3, FR-PAN-6, FR-PAN-10, FR-PAN-12). The term FR-PAN-3 stands for PA-based NP flame retardant with a molar ratio of PA to urea of 1:3.

Dipping of poplar specimens

The wood sample was dried at 103 °C for 8 h until it reached a constant mass (m_0). The wood was impregnated with 20% PA, FR-PAN-3, FR-PAN-6, FR-PAN-10, and FR-PAN-12 solutions under vacuum at -0.1 MPa for 2 h, then dried in an oven at 103 °C for 24 h to a constant weight (m). Treated and untreated wood was dried and balanced at the same temperature (25 ± 2 °C) and humidity ($65 \pm 3\%$) for a week. The weight gain rate of the poplar sample was calculated using Eq. 1 (Chen *et al.* 2021).

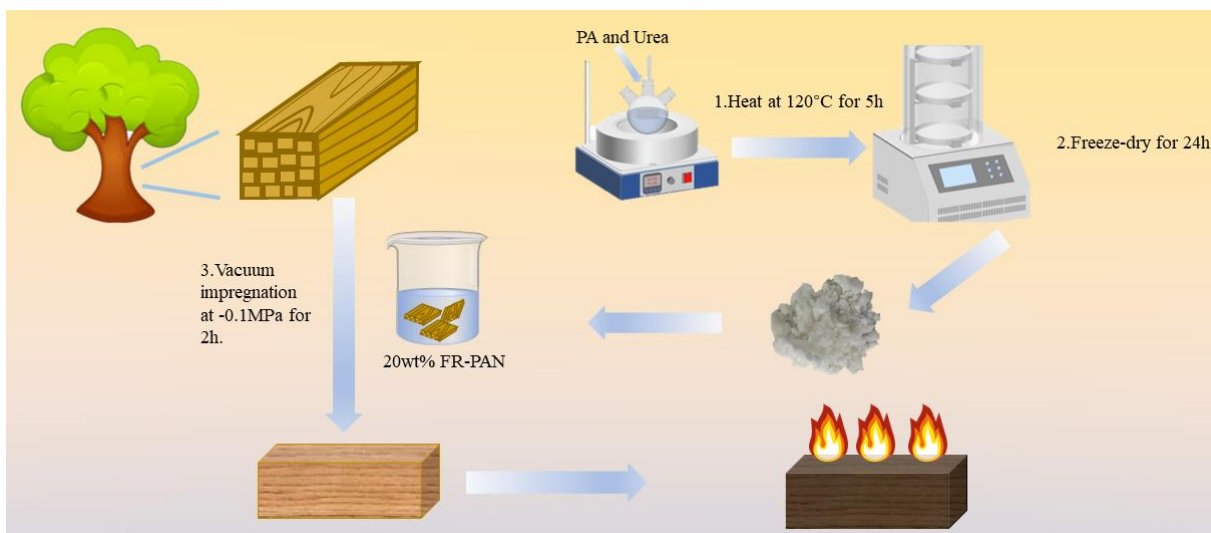$$WPG(\%) = (m - m_0)/m_0 * 100\% \tag{1}$$

Fig. 1. Preparation process

Fire Retardancy of the FR-PAN Modified Wood

The limiting oxygen index (LOI) of 10 samples in each group was tested, and the results were averaged. The samples were tested according to the GB/T2406.2-2009 standard. The sample size was 130 mm × 6.5 mm × 3 mm. For the smoke density test (SDR) according to GB/T8627-2007 standard, the sample size was 25 mm × 25 mm × 5 mm, and each group has 15 replicates. For the cone calorimetry test (CCT), the cone calorimeter (FTT00007, FTT, UK) was used to measure the combustion of the treated wood according to ISO5660-2, the sample size was is 100 mm × 100 mm × 20 mm, and radiation power was is 50 kW/m^2 . The indexes including heat release rate (HRR), total heat release (THR), smoke release rate (SPR), total smoke release (TSR), fire spread index (FGI), and residual mass (Residue) were taken into consideration.

Thermogravimetric and Thermodynamic Analysis

To explore the influence of FR-PAN on the thermal degradation process of wood, three different heating rates were employed under the N_2 atmosphere, and its activation energy was calculated according to the Kissinger method to study its degradation changes. The thermal degradation behavior of flame retardants was measured from 30 to 700 °C using a thermogravimetric analyzer (TGA Q5000, TA Instruments, USA) under N_2 atmosphere at heating rates of 5, 10, or 20 °C /min. The activation energy (E_a) required for the decomposition of the wood sample was calculated from the TG curve (5, 10, 20 °C/min) according to Eq. 2 (Hendrix *et al.* 1972),

$$\ln(\frac{\beta}{T_{pi}^2}) = \ln(\frac{A_K R}{E_K}) - \frac{E_K}{R}\frac{1}{T_{pi}} \tag{2}$$

where A and T_{pi} are the characteristic temperatures corresponding to the frequency factor and the maximum weight loss rate, respectively. R is the gas constant and β is the heating rate. For different heating rates, the activation energy E_a and frequency factor A are obtained by the slope and intercept of the curve for $1/T_{pi}$.

Residue Char Analysis

The residual char was used after the CCT. After 20 s of gold plating, the surface 5 mm char layer was observed in cross-section with SEM. The surface morphology of the sample was observed by cold field emission scanning electron microscope (Hitachi S-4800, Hitachi). X-ray photoelectron spectroscopy (XPS) was conducted through an XSAM 800 spectrometer (Kratos Co., Stretford, UK $h\gamma$=1486.6eV), using Al Kα excitation radiation, 12 kV operating voltage, and 15 mA working current selected for this test. A Raman microscope (Renishaw in Via, UK) excited at 514.5 nm was used to measure the peak cumulative area ratio R at 1350 cm^{-1} (peak D) and 1580 cm^{-1} (peak G). The smaller the R-value, the higher the graphitization degree of the residual char. Six kinds of residue char powder were laid in the grooves of monocrystal silicon sheet and tested by polycrystalline X-ray diffractometer (XRD-6, Beijing Spectrometer). The operating voltage of the instrument was 36 kV, the current was 20 mA, and the scanning range was 2θ=5° to 70°. The scanning speed was 4°/min. The degree of graphitization was calculated using CuKa1 radiation (λ= 0.15406 nm) and according to the Mering and Maire equations (Eqs. 3 and 4). The distance $d_{(002)}$ can be calculated from Bragg Eq. 4,

$$g = \frac{0.3440 - d_{(002)}}{0.3440 - 0.3354} \tag{3}$$

$$d_{(002)} = \frac{\lambda}{2sin\theta} \tag{4}$$

where 0.3440 nm is the layer spacing of a completely ungraphitized char layer, and 0.3354 nm is the ideal layer spacing of graphite crystals. The quantity $d_{(002)}$ is the layer spacing of the main characteristic peak of graphite (002 crystal face). λ is the incident wavelength, θ is the diffraction angle of the 002-crystal face, and the g value indicates the degree of graphitization of this char layer.

RESULTS AND DISCUSSION

Fire Retardancy
LOI and SDR analysis

The fire safety of poplar treated with FR-PAN was assessed by conducting tests of LOI and SDR. Table 1 presents the impact of FR-PAN on the LOI value and SDR of Poplar. The untreated group exhibited an LOI value of only 18.6%, indicating high flammability and emphasizing the necessity for flame retardant treatment. The introduction of phosphorus and nitrogen in PAN-6 groups resulted in a significant increase in LOI to 49.6%, representing a remarkable enhancement of 172% compared to the untreated group. Table 1 reveals that PA treatment led to a smoke density grade of 43.5. However, incorporation of urea reduced smoke emission, as evidenced by the lower smoke density grade (32.4) observed in the PAN-6 group, demonstrating a reduction by 72% compared to PA treated. The findings highlight the synergistic effect between phytic acid and urea, wherein the introduction of urea significantly improves poplar's flame retardancy while inhibiting smoke release. However, excessive addition of urea can lead to increased smoke release. It is well known that the smoke is very harmful to personnel safety in a fire, and the PAN-6 group shows a lower SDR, which will reduce the harm of smoke to personnel.

Table 1. Weight Gain Rates of the Modified Wood and their LOI and SDR

Group	WPG(%)	LOI(%)	SDR
Control	-	18.6±0.1	7.72±3.02
PA	18.2±1.2	39.8±0.1	43.5±3.69
PAN-3	21.3±0.85	40.2±0.1	36.7±2.49
PAN-6	22.1±1.34	49.6±0.1	28.4±1.65
PAN-10	22.9±0.96	59.4±0.1	37.5±1.43
PAN-12	21.8±1.34	57.3±0.1	36.1±1.14

CCT Analysis

CONE testing is commonly employed for laboratory-scale evaluation of fire parameters and is widely acknowledged as an effective method for regulating the burning behavior of real fires. During the test, various parameters were determined (refer to Fig. 2): Heat release rate (HRR), Total heat release (THR), Total smoke rate (TSR), Smoke production rate (SPR), and residual mass, with corresponding data listed in Table 2. As depicted in Fig. 2, at the initial stage of the test, the untreated wood group exhibited a sharp increase in HRR due to surface wood combustion. After 200 s, a char layer formed on the surface leading to isolation of oxygen and heat, resulting in a constant HRR value. At around 480 s, rupture of the surface char layer caused renewed pyrolysis from internal

wood components, reaching a PHRR of 372 kW/m^2 at 569s (Table 2). After 800 s, the heat release decreased because the wood smoldered, and the final char residue was 5.9%.

As shown in Fig. 2 (b), it is evident that the flame retardant treatment significantly altered the THR and TSR of poplar wood. The addition of urea in PAN-6 group resulted in a remarkable reduction of 57.1% and 82% in THR compared to untreated group and PA treated group, respectively, indicating the effective suppression of heat release by urea addition. Table 2 demonstrates a trend where the THR decreased with increasing urea content. This can be attributed to the molten state of urea at temperatures around 150 °C due to its polar nature, which facilitates enhanced contact between ammonium phytate and cellulose/hemicelluloses (Cheng *et al.* 2022). At temperatures above 160 °C, decomposition reactions occur, leading to ammonia release from urea decomposition as well as pyrophosphoric acid formation from FR-PAN degradation catalyzing dehydration reactions converting cellulose/hemicellulaceous residues. Additionally, pyrophosphoric acid promotes expansive six-char ring structures on phytic acid groups, effectively providing thermal insulation properties while inhibiting smoke emission and toxic gas production (Hendrix *et al.* 1972). The wood combustion process begins at the ignition point temperature, heat accumulation was necessary to reach the ignition point temperature, and a lower THR will reduce the fire hazard. The PAN-6 group exhibited an impressive final residue char amount, that was about 4.9 times higher than that observed for untreated group at the end of the experiment (32.4%). The increase of residual char not only means a decrease in total heat release, but also a continuous and dense char layer has a certain mechanical strength, which can delay or even change the collapse of indoor furniture and building structures, which was very important in fire safety. These findings demonstrate excellent flame retardancy performance achieved through FR-PAN-6 treatment.
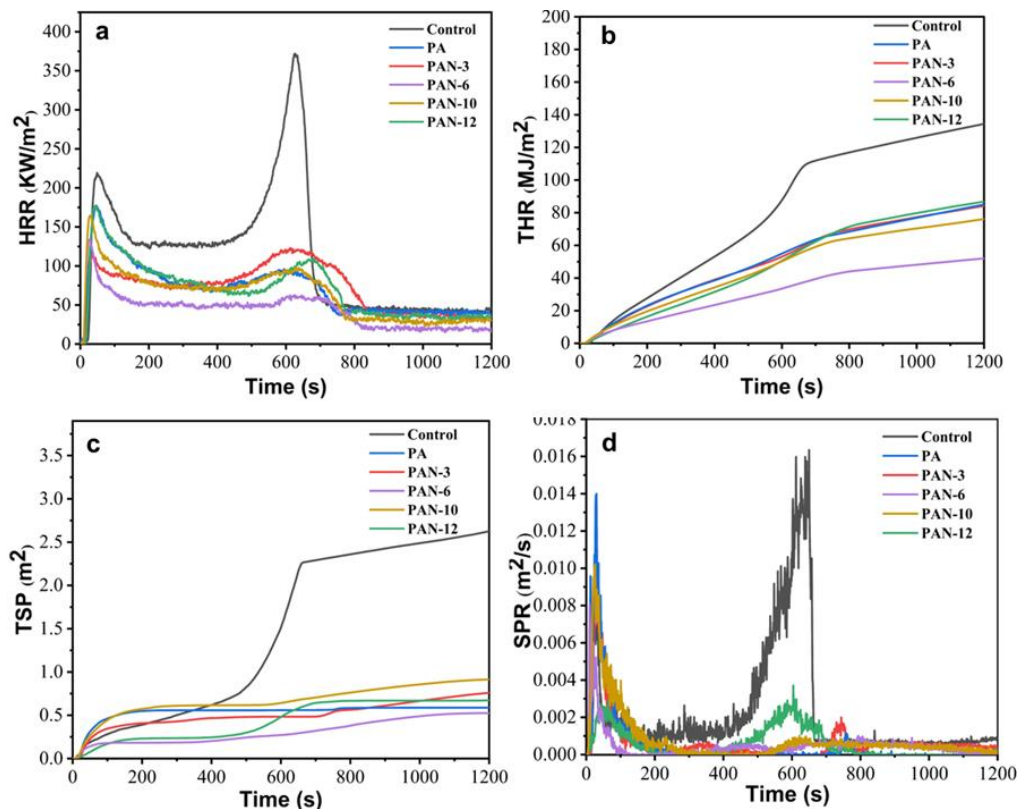

Fig. 2. HRR(a), THR(b), TSR(c), and SPR(d) plots of wood samples

Table 2. Combustion Parameters of Modified Wood Samples

Group	FGI	PHRR (kW/m^2)	THR (MJ/m^2)	TSR (m^2/m^2)	PSRR (m^2/s)	Residue (%)
Control	0.054	371.89	121.37	295.35	0.0163	5.9
PA	0.107	177.28	85.03	85.34	0.0142	30.1
PAN-3	0.092	177.67	84.2	66.04	0.0122	30.59
PAN-6	0.067	134.36	52.02	59.08	0.0055	32.41
PAN-10	0.089	123.00	86.80	72.37	0.0081	29.19
PAN-12	0.048	164.61	92.72	102.75	0.0102	26.92

Note: PHRR (peak of heat release rate)

As shown in Fig. 2 (d), the SPR of the treated group was significantly reduced compared to untreated and PA-treated groups. Specifically, the SPR of the PAN-6 group was 0.0081m^2/s, which was 50.3% and 42.95% lower than that of untreated and PA treated group. Furthermore, Fig. 2 (c) illustrates that TSR of PAN-6 group decreased by 80.0% and 30.8% compared to untreated and PA treated group. The addition of urea improved the smoke suppression performance of flame-retardant treated group by decreasing the PHRR value initially and then increasing it later. When there was excess urea in the system, urea decomposes at 170 °C to generate NH$_3$ and HCNO (Eq. 5) (Ana *et al.* 2015), and ammonia expands the char-containing char layer, which can form a physical barrier to isolate the entry of oxygen and heat. This will protect the substrate and reduce heat release. On the other hand, the HCNO generated reacts with the hydroxyl groups in cellulose and hemicellulose to form a carbamate group (Eq. 6) (Geake *et al.* 2020), which causes a decrease in the crystallinity of cellulose and accelerates the decomposition of glycosyl units (Hassan *et al.* 2010). This results in reduced heat release and smoke release. When the urea content was excessive, the expansive structure was destroyed, and the thermal and oxygen insulation ability of the surface char layer was reduced, resulting in the reduction of flame retardant and smoke suppression performance. Overall, when considering THR and TSR, treated groups with added urea demonstrate superior flame retardant properties compared to both untreated samples and those treated with PA alone. Notably, a molar ratio of phytic acid to urea at 1:6 resulted in an expansion structure that efficiently suppressed smoke generation while minimizing heat release.

$$CO(NH_2)_2 \rightarrow NH_3 \uparrow + HCNO \qquad (5)$$

$$R_1\text{-}N\text{=}C\text{=}O + R_2\text{-}OH \rightarrow R_1\text{-}NH\text{-}CO\text{-}O\text{-}R_2 \qquad (6)$$

Based on this mechanism, Fig. 3 shows the plot of THR relative to mass loss, as they relate to the basic properties of the group such as combustion efficiency and effective heat of combustion of volatiles. There was a linear fit to the mean value, and the slope of the poplar curve treated with phytic acid and ammonium phytate changed significantly. This effect may be related to the gas phase effect, while the large decrease in the mass loss value indicates the flame retardant effect of the condensed phase. The effective combination of gas-solid flame retardants was mainly attributed to the P-N synergistic effect of the FR-PAN. The corresponding parameters are shown in the table, among which the slope of PAN-6 group was the smallest, which means that its P-N synergistic effect was the best.
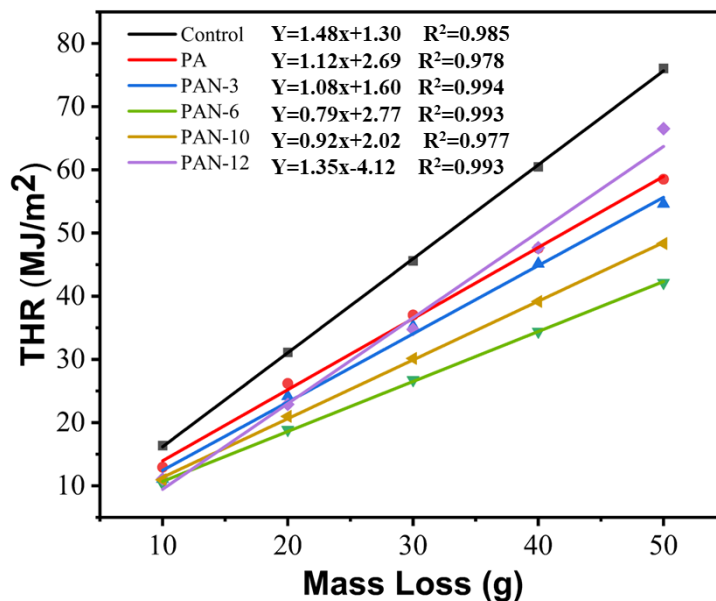
Fig. 3. Fitting of moss loss and total heat release of the FR-PAN modified wood

TGA and Thermodynamic Analysis

The pyrolysis process of poplar wood can be observed in Fig. 4 (a). As shown, the process can be divided into three stages. The first stage (30 to 237 °C) involved evaporation of water and heat-sensitive volatiles from the poplar wood, resulting in a mass loss of 4%. During the second stage (237 to 394 °C), approximately 70% mass loss took place as cellulose and hemicellulose decompose extensively, forming small molecular organic matter (Xiong *et al.* 2019). The third stage (394 to 700 °C) exhibited a mass loss of about 11%, indicating completion of half fiber and cellulose decomposition. Lignin primarily decomposes into aldehydes and forms char at this stage, resulting in a final residue char level of 15.0%.

As shown in Fig. 4(b), the degradation process of treated groups also can be categorized into three stages. In the initial stage (30 to 150 °C), there was a mass loss of 5%, mainly attributed to water volatilization and release of heat-sensitive substances. The second stage (150 to 290 °C) experienced an approximate mass loss of 45%, with an initial decomposition temperature falling between untreated wood and PA-treated group. The initial decomposition temperature of the untreated group in Table 3 exhibited an initial increase followed by a decrease upon addition of urea, with PAN-6 group displaying the highest maximum initial decomposition temperature at 170.4 °C. This higher temperature suggests an improved thermal stability of the treated group.

In Fig. 4 (b), a distinct peak was observed at 190 °C on the DTG curve, which differed from both the untreated and PA-treated groups. Within this temperature range, heat absorption by the ammonium phosphate group leads to the generation of ammonium dihydrogen phosphate, while ammonium pyrophosphate releases non-combustible gases such as CO_2, NH_3, and water vapor (Chen *et al.* 2010). These sequential reactions inhibit combustible gas production. Furthermore, the DTG curve for the PAN-6, PAN-10, and PAN-12 groups showed strong peaks at 258, 253, and 249 °C, respectively, indicating the phosphorylation reaction on C-6 hydroxyl groups of dehydrated glucose (Puziy *et al.* 2006). During the third stage (290 to 700 °C), a mass loss of approximately 19% occurs primarily due to lignin degradation and char formation. Among all the five flame retardant

treated wood examined here, PAN-6 group exhibited a residue char level of about 41.6% at 700 °C representing the highest value thereby indicating an enhanced thermal stability of its residue char. As shown in Table 3, with increasing urea concentration there is a gradual decrease in activation energy during thermal decomposition for treated groups. This trend can be attributed to high urea concentrations. After calculation, it was found that the amount of urea added had a certain effect on the activation energy of the reaction, and when the urea content was excessive, it would cause the activation energy to decrease, which was consistent with the findings of Nam *et al*. (2011).

The above discussion demonstrates that the flame retardancy and thermal stability of treated groups were significantly enhanced compared to untreated and PA-treated group, which can be attributed to the incorporation of urea.
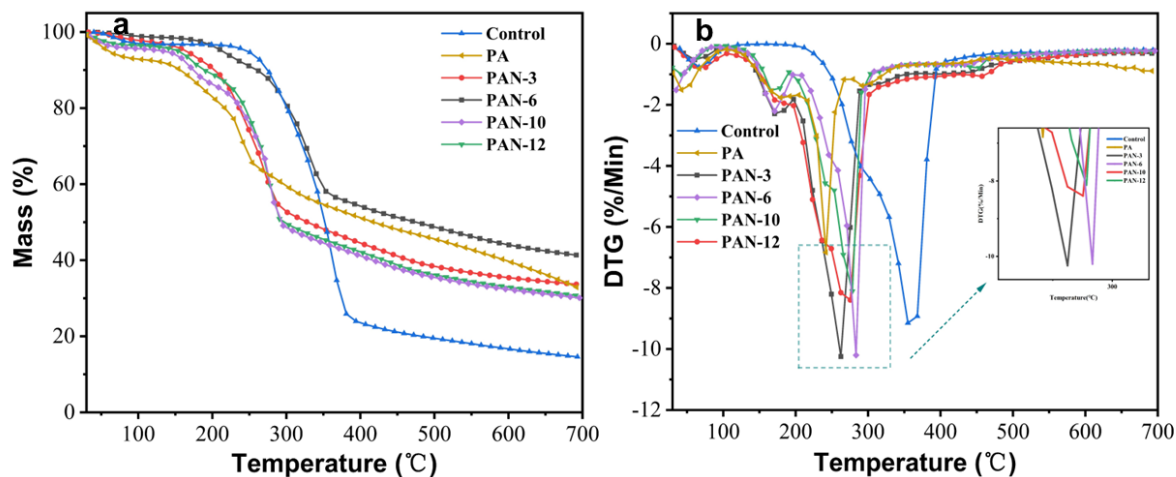

Fig. 4. Thermal behavior of untreated and treated wood, TG (a) and DTG (b) curves

Table 3. Thermogravimetric Data and Thermodynamic Parameters of Wood Samples in N_2

Group	E_a(kJ/mol)	$T_{5\%}$	Residue at 700°C (%)	T_{max}	R^2
Control	156.91	260.81	14.96	358.98	0.9959
PA	52.95	59.62	32.9	241.72	0.9746
PAN-3	108.08	164.88	33.67	275.37	0.9965
PAN-6	72.05	170.38	41.61	278.39	0.9941
PAN-10	52.02	134.19	30.01	281.64	0.9985
PAN-12	47.68	143.45	30.17	262.44	0.9893

Note: E_a = reaction activation energy, unit KJ/mol

$T_{5\%}$ = initial decomposition temperature, unit $^\circ$C

Percentage of residue char at 700 °C, unit %

T_{max} = The characteristic temperature corresponds rate, unit $^\circ$C

Residual Char Graphitization Analysis

SEM analysis

As shown in Fig. 5, the action mechanism of flame retardants, the residue char in wood samples after combustion was analyzed. Figure 5 presents the residual cell wall thickness of both treated and untreated wood samples. When fully burned, the untreated

group exhibited minimal residual cell wall thickness of only 0.9 um. In contrast, the PAN-6 group formed a protective expansion structure during combustion that restricted heat and gas transfer and prevented rapid pyrolysis within the wood, resulting in highly graphitized residue char production. The residual cell wall thickness measured 2.09 um for treated group, which was twice that observed in untreated group. There was a relationship between urea addition and residual cell wall thickness in the treatment group. Specifically, there was pattern of an initial increase followed by a decrease, consistent with CCT results.
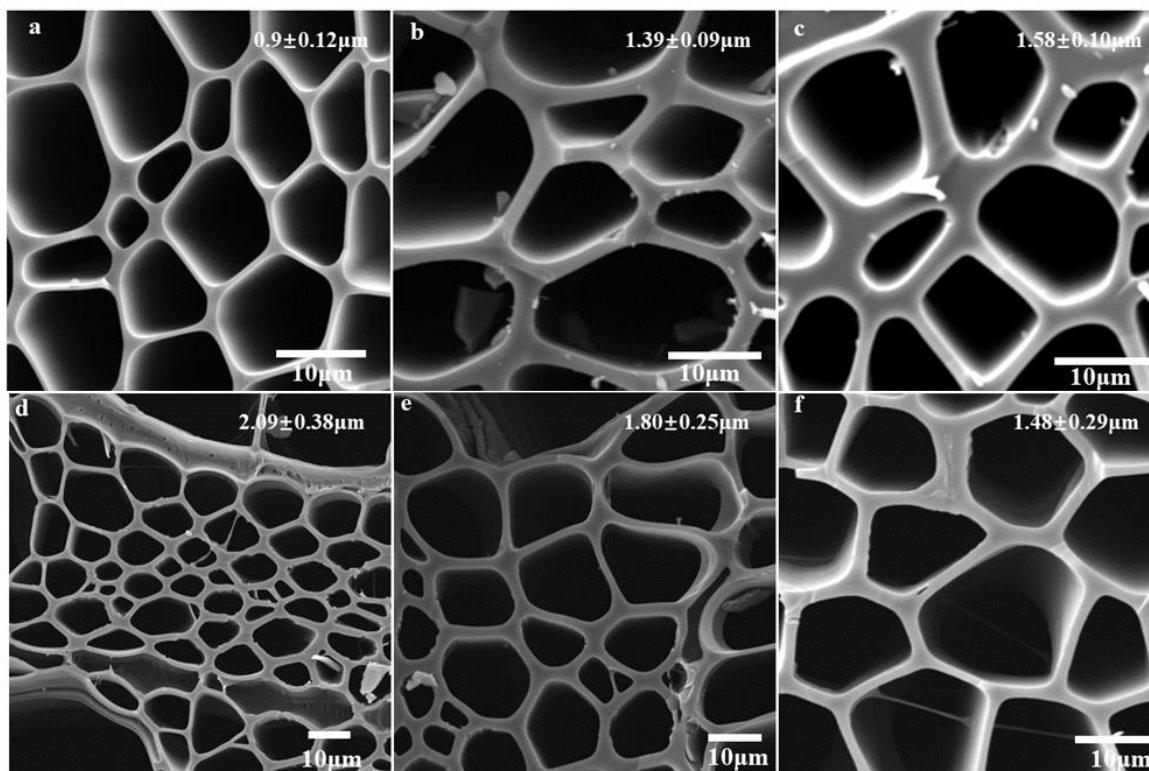
Fig. 5. Morphology of residues char obtained from CCT. a, b, and c represent the control, PA, and PAN-3 group, and d, e, and f represent PAN-6, PAN-10, and PAN-12 group. (Insert: Residual thickness of the cell wall).

Raman and XRD Analysis

Raman spectroscopy was employed to evaluate char graphitization degree as more graphite structures within char residues indicate higher thermal stability (Lin *et al.* 2018). Figure 6 displays two prominent peaks observed at 1350 cm^{-1} (disordered char structure or D-band) and 1580 cm^{-1} (graphitized char structure or G-band). The peak area ratio ($R=I_D/I_G$) between D-band and G-band is commonly used as an indicator for graphitization degree assessment. As shown in Fig. 6, for untreated group, ID/IG value measured at 3.32. In comparison, the flame-retarded group exhibited a significantly reduced ID/IG value (1.91), suggesting that FR-PAN contributes to highly graphitized char formation. Table 4 illustrates ID/IG values for both treated and untreated group. The values followed a trend similar to scanning electron microscopy rule regarding residual cell wall thickness.

Table 4. Residual Char Graphitization Parameters

Group	XRD(2θ)	$d_{(002)}$/nm	g	Roman(AG)	Roman(AD)	R
Control	22.58	0.410	-5.74	5.79*103	1.92*104	3.32
PA	23.02	0.392	-4.89	7.23*103	2.22*104	3.07
PAN-3	23.12	0.385	-4.77	2.03*103	6.08*103	2.99
PAN-6	23.56	0.375	-3.87	8.42*103	1.61*104	1.91
PAN-10	23.54	0.383	-3.91	4.13*103	1.02*104	2.46
PAN-12	23.48	0.379	-4.12	2.23*103	5.78*104	2.59

The 2θ values of the untreated and treated groups, as presented in Table 4, are recorded as follows: 22.58°, 23.02°, 23.12°, 23.14°, 23.56°, 23.54°, and 22.68° respectively. Correspondingly, the d(002) values for these groups were measured as: 0410, 0.392, 0.385, 0.384, and 0.375 nm, respectively. The g values obtained for both treated and untreated group were found to be -5.74, -4.89, -4.77, -4.60, -3.87, and -3.91, respectively. It has been shown that FR-PAN can contribute to the formation of highly graphitized char. Additionally, the graphitization degree of residue char initially increased with the addition of urea but then decreased. This trend is consistent with the findings from laser Raman testing.
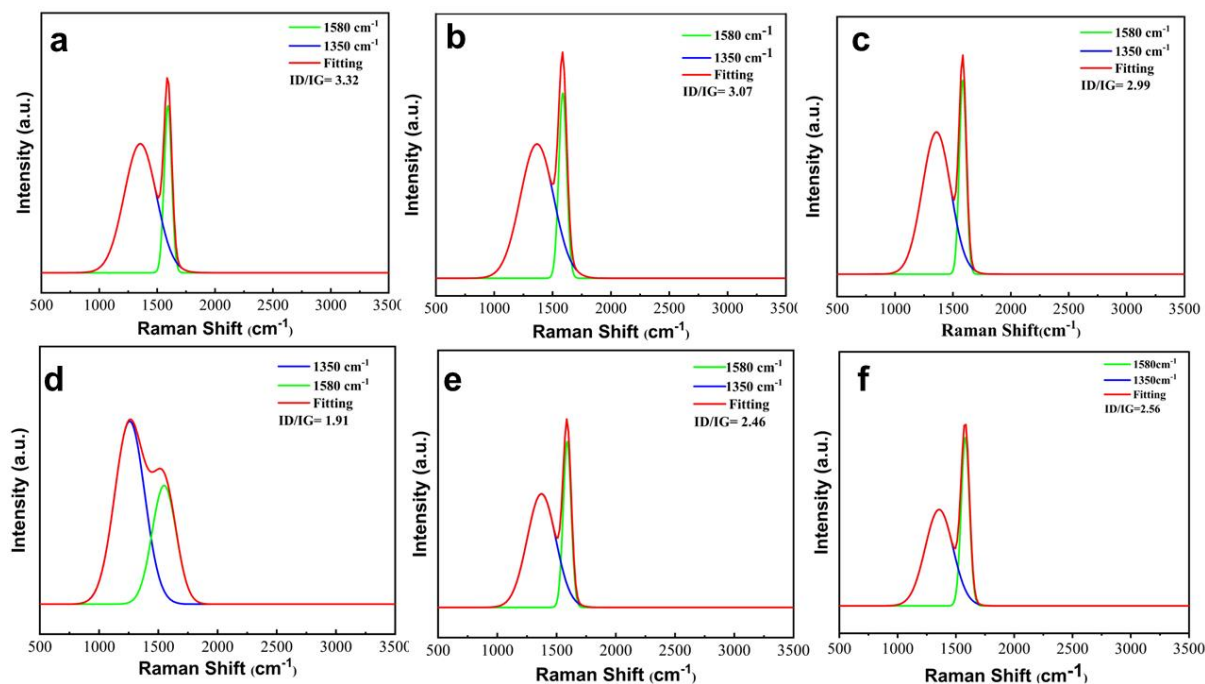
Fig. 6. Raman spectra of different coal and coke residues. a, b, and c represent the control, PA, PAN-3 group, and d, e, f represent PAN-6, PAN-10, PAN-12 group.

XPS Analysis

Elemental composition analysis was conducted using the XPS technique. Figure 7 displays high-resolution XPS spectra of C1S. Peak assignments along with their corresponding contributions can be found in Table 5. Notably, the C content in untreated wood was observed to be higher than that in treated group because only the black characeous portion of the residue was sampled. Moreover, a significant increase in peak

intensity at around 285.2 to 285.8 eV was observed after flame retardant treatment. This suggests a greater presence of C-P/C-N/C-O-P structures being formed (Wang *et al.* 2020). Comparatively, the concentration of C-P/C-N/C-O-P within PAN-6 group char residues (19.0%) exceeded that present in untreated wood (16.5%). This change in C1s peak confirms the introduction of phosphorus into the char skeleton during combustion (Freitas 2006).

In the O1S spectrum, P=O, which denotes the existence of polyphosphates in the residues char, can be seen in the O1S spectrum. P-O-C, which denotes the creation of cross-linked structures, can be seen in the O1S spectra of the flame-retardant treated group. P=O (13.6%) and C-O-P (6.2%) concentrations in the residues char of the PAN-6 group were much greater than those of the untreated groups. As shown in Table 5, the matching peaks of pyrrole/pyridinium nitrogen (N-5) and pyridinium nitrogen (N-6) occurred in the XPS energy spectra of the residues char following flame retardant treatment (Théotime *et al.* 2022). N-Q concentration in the coke of groups treated with flame retardants (2.67%) was significantly greater than that of the residue char of PA treated group (0.86%), which indicates that more N is injected into the graphite structure. Nitrogen doping in the char structure considerably improves the stability of the residue char.
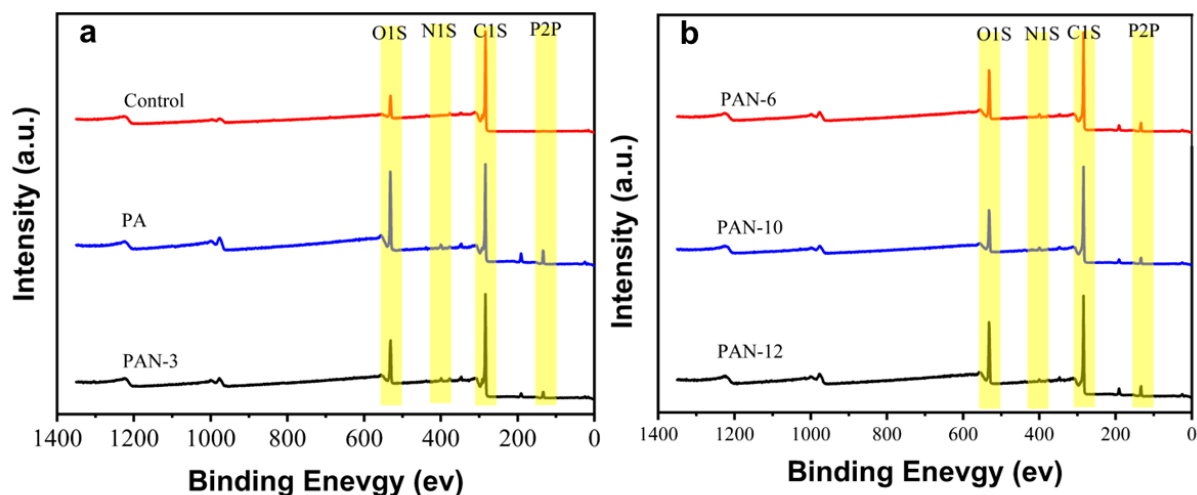

Fig. 7. XPS scans of different residues char at CCT

The P-C/P-O/P=O structure and P_2O_5 showed peaks in the P2P spectrum (Table 5) at around 134 and 135 eV, respectively. Compared to untreated group and PA treated group, treated group has a higher P-C/P-O/P=O structural content (Théotime *et al.* 2023). The amount of P (88.1%) in the residual char was accounted for by the P-C/P-O/P = O structure present in the treated group char in the PAN-6 group, which had a 3.97% content. The amount of untreated group residue char was less than 0.5%. High stability the PAN-6 group charring layer can considerably increase wood flame resistance (Yu *et al.* 2021). In general, the addition of P and N elements during the combustion of flame-retardant-treated group can significantly enhance the flame-retardant performance. The highest content and best residual char stability were produced when the molar ratio of phytic acid to urea was 1:6, which resulted in the formation of P = O, P-C/P-O/P=O, and other hybrids.

The introduction of phytic acid in the combustion process led to the successive generation of metaphosphoric acid, phosphoric acid, polymetaphosphoric acid, and pyrophosphoric acid. Finally the glycan unit is dehydrated into charcoal under the action

of phosphorus-containing compounds to generate polyphosphate (Fig. 7), and P and N are introduced into the char layer (Maoyuan *et al.* 2019; Li *et al.* 2020). Doping P and N can improve the thermal oxidation stability of the char layer. The doping of heteroatoms reduces the reactivity of the char active center (Liew *et al.* 2016). It also plays a role in inhibiting the gasification of the char layer, enhances the structural integrity of the char layer, and promotes the formation of porous thermal insulation char layer in the condensed phase, thereby enhancing the flame retardancy and smoke suppression. The application of adsorption, filtration and indoor insulation groups will be expanded.

Table 5. Peak Assignments for C1S, O1S, N1S, and P2P Spectra of Different Coke Char Residues Obtained from CCT

Group	Component	Control	PA	PAN-3	PAN-6	PAN-10	PAN-12
C1S *	C-C/C-H C=O/C-N	57.03 8.6	36.50 8.9	48.71 9.13	43.87 4.65	43.92 7.5	47.58 3.62
	C-O/C-P/C-N	16.51	7.25	9.05	19.01	10.39	8.48
	O=C-O	6.86	8.60	6.57	5.11	13.8	9.19
O1S	O-C/P-O-C O=C/O=P	4.65 2.78	13.23 15.96	8.33 12.37	6.24 13.63	4.93 13.10	7.66 15.33
	O+H_2O	2.83	-	-	-	-	-
N1S	N-5 N-6	- -	0.73 0.071	- 0.11	- 0.32	- 0.64	- 0.55
	N-Q	-	0.86	1.71	2.37	1.95	1.10
	N-X	-	-	0.031	-	-	-
P2P	P-C/P-O/P=O P_2O_5		5.12 2.28	3.11 0.88	3.97 0.54	2.73 1.03	4.68 0.8

*The data were analysed by Avantage software

Flame-Retardant Mechanism

According to the above analysis, the flame retardant mechanism of FR-PAN may be summarized as follows. In the combustion process, FR-PAN is decomposed by heat to produce NH_3 and H_2O, which will dilute the combustible gas in the gas phase. In addition, the phytic acid group will also generate P • and PO • radicals, which will inhibit the combustion chain reaction. When urea is present in the flame retardant system, urea becomes molten when heated at 150 °C to 170 °C, promotes the contact between FR-PAN and hemicellulose and cellulose, and accelerates the phosphoric acid to catalyzed the dehydration of hemicellulose and cellulose into char. In addition, NH_3 and HCNO produced by the decomposition of urea, and the NH_3 will promote the formation of a char layer with an expansive structure, which will contribute a good flame retardant effect in the condensed phase. The dehydration will reduce the crystallinity of cellulose and promote the decomposition of cellulose. Finally, nitrogen and phosphorus are introduced into the char layer, and the addition of heteroatoms will improve the thermal oxidation stability of the char layer, which can effectively inhibit the release of combustibles and smoke. The results showed that when the molar ratio of phytic acid to urea was 1:6, the flame retardancy and smoke suppression performance of this treated group was the best.
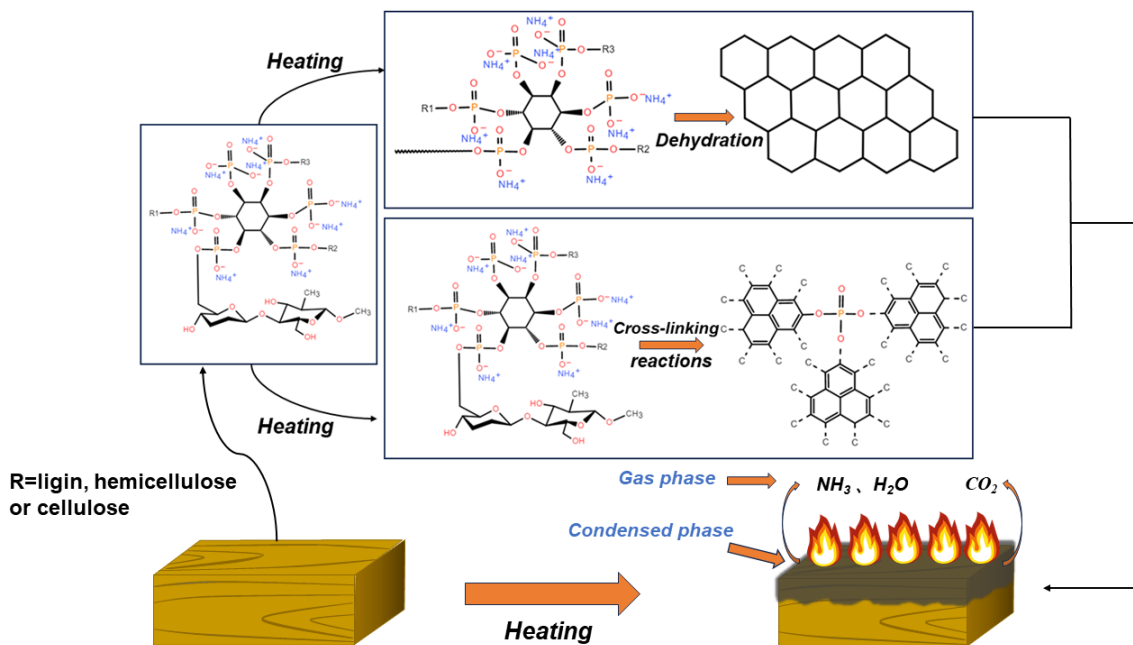
Fig. 8. Schematic diagram of wood-FR-PAN flame retardant mechanism

CONCLUSIONS

1. Phytic acid (PA) can react with urea in the liquid phase to form a new green and efficient phosphorus-nitrogen synergistic flame retardant, which can be attached to the wood cell wall by vacuum impregnation to achieve flame retardancy. The results showed that the phytic acid-based NP fire retardant (FR-PAN) had obvious flame retardant and smoke suppression effect on poplar. It was able to effectively increase the lower oxygen index (LOI) of flame retardant poplar samples, which increased to 59.4% in the PAN-10 group.

2. In the cone calorimetry test (CCT) experiment, peak of heat release rate (PHRR) of the PAN-6 group was reduced by 63.8% compared with pure poplar, the total heat release (THR) decreased by 57.14%, TSR per unit area was reduced by 80.0%, showing excellent flame retardant and smoke suppression properties.

3. During the decomposition process, FR-PAN releases non-combustible gases, and pyrophosphate like substances produced promote the dehydration of hemicellulose and cellulose to produce more coke. When PA:urea = 1:6, highly graphitized phosphorus and nitrogen doped char was formed, which played an important role in improving the flame retardant smoke suppression performance of FR-PAN.

ACKNOWLEDGMENTS

Author Contributions Statement

Q. S. wrote the main manuscript, C. D. was responsible for data curation, S. X. and L.Y. performed formal analysis, S. X. supplied the resources and came up with the methodology, S. L. were responsible for funding acquisition, methodology, and project administration. All authors reviewed the manuscript.

Declaration of Competing Interest

The authors declare that they have no known competing financial interests or personal relationships that could have appeared to influence the work reported in this paper.

Data Availability Statements

The datasets generated during and/or analysed during the current study are available from the corresponding author on reasonable request.

REFERENCES CITED

Attia, N., Ahmed, H., Yehia, D., Hassan, M., and Zaddin, Y. (2016). "Novel synthesis of nanoparticles-based back coating flame-retardant materials for historic textile fabrics conservation," *Journal of Industrial Textiles* 46(6), 1379-1392. DOI: 10.1177/1528083715619957

Chen, C., Kuang, Y., Zhu, S., Burgert, I., Keplinger, T., Gong, A., Li, T., Berglund, L., Eichhorn, S. J., and Hu, L. (2020). "Structure–property–function relationships of natural and engineered wood," *Nature Reviews Materials* 5, 1-25. DOI: 10.1038/s41578-020-0195-z

Chen, G., Chaoji, C., Pei, Y., He, S., Liu, Y., Jiang, B., Jiao, M., Gan, W., Liu, D., Yang, B., and Hu, L. (2019). "A strong, flame-retardant, and thermally insulating wood laminate," *Chemical Engineering Journal* 383, article 123109. DOI: 10.1016/j.cej.2019.123109

Chen, H., Ferrari, C., Angiuli, M., Yao, J., Raspi, C., and Bramanti, E. (2010). "Qualitative and quantitative analysis of wood samples by Fourier transform infrared spectroscopy and multivariate analysis," *Carbohydrate Polymers* 82, 772–778. DOI: 10.1016/j.carbpol.2010.05.052

Chen, Z., Zhang, S., Ding, M., Wang, M., and Xu, X. (2021). "Construction of a phytic acid–silica system in wood for highly efficient flame retardancy and smoke suppression," *Materials* 14, article 4164. DOI: 10.3390/ma14154164

Cheng, Y.-W., Gu, C.-G., Wang, J.-T., Yang, X.-L., Bian, Y.-R., and Xin., J. (2015). "Recent advances in mechanism and processes of microbial degradation of polybrominated diphenyl ethers," *Environmental Chemistry* (04),637-648, article 100049. DOI:10.7524/j.issn.0254-6108.2015.04.2014031407

Cheng, X. W., Wu, Y. X., Huang, Y. T., Jiang, J. R., and Guan, J. P. (2020). "Synthesis of a reactive boron-based flame retardant to enhance the flame retardancy of silk," *Reactive and Functional Polymers* 156, article 104731. DOI: 10.1016/j.reactfunctpolym.2020.104731

Cheng, X., Shi, L., Fan, Z., Yu, Y., and Liu, R. (2022). "Bio-based coating of phytic acid, chitosan, and biochar for flame-retardant cotton fabrics," *Polymer Degradation and Stability* 199, article 109898. DOI: 10.1016/j.polymdegradstab.2022.109898

Dhineshbabu, N. R., Manivasakan, P., Karthika, A., and Rajendran, V. (2014).

"Hydrophobicity, flame retardancy and antibacterial properties of cotton fabrics functionalised with MgO/methyl silicate nanocomposites," *RSC Advances* 4, 32161-32173. DOI: 10.1039/c4ra03348e

Fan, C., Gao, Y., Li, Y., Yan, L., Zhu, D., Guo, S., and Wang, Z. (2022). "A flame-retardant densified wood as robust and fire-safe structural material," *Wood Science and Technology* 57(1), 111-134. DOI: 10.1007/s00226-022-01415-9

Freitas, A. (2006). "Polymer degradation and stability," *Polymer Science* 87, 171-181. DOI:10.1016/j.polymdegradstab.2004.10.003

Gebke, S., Thümmler, K., Sonnier, R., Tech, S., Wagenfuhr, A., and Fischer, S. (2020). "Flame retardancy of wood fiber materials using phosphorus-modified wheat starch," *Molecules* 25(2), article 335. DOI: 10.3390/molecules25020335

Giraud, S., Rault, F., Rochery, M., and Gacquere, L. (2013). "Use of bio-based carbon source to develop intumescent flame retardant polyurethane coating for polyester textile fabric," in: *Proceedings of the 14th European Meeting on Fire Retardant Polymers*, FRPM13.

Grancaric, A. M., Botteri, L., Alongi, J., and Malucelli, G. (2015). "Synergistic effects occurring between water glasses and urea/ammonium dihydrogen phosphate pair for enhancing the flame retardancy of cotton," *Cellulose* 22, 2825-2835. DOI: 10.1007/s10570-015-0671-6

Hassan, M. A., Kozlowski, R., and Obidzinski, B. (2010). "New fire-protective intumescent coatings for wood," *Journal of Applied Polymer Science* 110(1), 83-90. DOI: 10.1002/app.28518

Hendrix, J. E., Drake, G. L., and Barker, R. H. (1972). "Pyrolysis and combustion of cellulose. II. Thermal analysis of mixtures of methyl-D-glucopyranoside and levoglucosan with model phosphate flame retardants," *Journal of Applied Polymer Science* 16, 41-59. DOI: 10.1002/app.1972.070160105

Li, F., Gui, X., Ji, W., and Zhou, C. (2020). "Effect of calcium dihydrogen phosphate addition on carbon retention and stability of biochars derived from cellulose, hemicellulose, and lignin," *Chemosphere* 251, article 126335. DOI: 10.1016/j.chemosphere.2020.126335

Li, L.M., Chen, Z., Lu, J., Wei, M., and Jiang, P. (2021). "Combustion behavior and thermal degradation properties of wood impregnated with intumescent biomass flame retardants: Phytic acid, hydrolyzed collagen, and glycerol," *ACS Omega* 6(5), 3921-3930. DOI: 10.1021/acsomega.0c05778

Li, T. T., Xing, M., Wang, H., Huang, S. Y., Fu, C., Lou, C. W., and Lin, J. H. (2019). "Nitrogen/phosphorus synergistic flame retardant-filled flexible polyurethane foams: Microstructure, compressive stress, sound absorption, and combustion resistance," *RSC Advances* 9, 21192-21201. DOI: 10.1039/C9RA02332A

Lin, D.-Q., Hu, C.-G., Chen, H., Qu, J., and Dai, L.-M. (2018). "Microporous N,P-codoped graphitic nanosheets as an efficient electrocatalyst for oxygen reduction in whole pH range for energy conversion and biosensing dissolved oxygen (*Chem. Eur. J.* 69/2018)," *Chemistry – A European Journal* 24(69), 18487-18493. DOI: 10.1002/chem.201802040

Lin, C. F., Karlsson, O., Martinka, J., Rantuch, P., Garskaite, E., Mantanis, G. I., and Sandberg, D. (2021). "Approaching highly leaching-resistant fire-retardant wood by in situ polymerization with melamine formaldehyde resin," *ACS Omega* (19), 12733-12745. DOI: 10.1021/acsomega.1c01044

Liu, Y., Zhao, J., Deng, C. L., Chen, L., Wang, D. Y., and Wang, Y. Z. (2011). "Flame-

retardant effect of sepiolite on an intumescent flame-retardant polypropylene system," *Industrial Engineering Chemistry Research* 50, 2047-2054. DOI: 10.1021/ie101737n

Liu, H., Wu, H., Song, Q., Zhang, J., Li, W., and Qu, H. (2020). "Core/shell structure magnesium hydroxide @ polyphosphate metal salt: preparation and its performance on the flame retardancy for ethylene vinyl acetate copolymer," *Journal of Thermal Analysis and Calorimetry* 141, 1341-1350. DOI: 10.1007/s10973-019-09131-6

Liu, Y., Zhang, A.-S., Cheng, Y.-M., Li, M.-H., Cui, Y.-C., and Li, Z.-W. (2023). "Recent advances in biomass phytic acid flame retardants," *Polymer Testing*. 124, article 108100. DOI:10.1016/j.polymertesting.2023.108100

Li, M., Lu, L., Dai, Z., Hong, Y., Chen, W., Zhang, Y., and Qiao, Y. (2019). "Enhanced ablation resistance of glass beads and ZrB_2 modified SiO_2 (f)-phenolic composites," *Materials Reports* 33(8), 1302-1306. DOI: 10.11896/cldb.19010181

Nam, S., Condon, B. D., Parikh, D. V., Zhao, Q., Cintrón, M. S., and Madison, C. (2011). "Effect of urea additive on the thermal decomposition of greige cotton nonwoven fabric treated with diammonium phosphate," *Polymer Degradation and Stability* 96, 2010-2018. DOI: 10.1016/j.polymdegradstab.2011.08.014

Puziy, A. M., Poddubnaya, O. I., and Ziatdinov, A. M. (2006). "On the chemical structure of phosphorus compounds in phosphoric acid-activated carbon," *Applied Surface Science* 252, 8036-8038. DOI: 10.1016/j.apsusc.2005.10.044

Song, K., Ganguly, I., Eastin, I., and Dichiara, A. (2020). "High temperature and fire behavior of hydrothermally modified wood impregnated with carbon nanomaterials," *J. Hazardous Materials* 384, article 121283. DOI: 10.1016/j.jhazmat.2019.121283

Tang, L., Wu, Y., Yuan, L., and Hu, Y. (2021). "The heat insulation and smoke suppression effect of M-Si-phosphocarbonaceous catalyzed by metal salt-doped APP silicon gel *in situ* build in wood," *Journal of Thermal Analysis and Calorimetry* 146(6), 2353-2364. DOI: 10.1007/s10973-020-10530-3

Théotime, B., Weiss-Hortala, E., and Nzihou, A. (2022). "Calcium as an innovative and effective catalyst for the synthesis of graphene-like materials from cellulose," *Scientific Reports* 12(1), article 21492. DOI: 10.1038/s41598-022-25943-3

Théotime, B., Weiss-Hortala, E., Lyczko, N., and Nzihou, A. (2023). "The mechanisms of calcium-catalyzed graphenization of cellulose and lignin biochars uncovered," *Scientific Reports* 13, article 11390. DOI: 10.1038/s41598-023-38433-x

Tong, J., Zheng, H., Fan, J., Li, W., Wang, Z. F., Zhang, H., Dai, Y., Chen, H., and Zhu, Z. (2023). "Fabricating well-dispersed poly(vinylidene fluoride)/expanded graphite composites with high thermal conductivity by melt mixing with maleic anhydride directly," *Polymers* 15(7), article 1742. DOI: 10.3390/polym15071747

Wang, K., Meng, D., Wang, S., Sun, J., Li, H., Gu, X., and Zhang, S. (2022). "Impregnation of phytic acid into the delignified wood to realize excellent flame retardant," *Industrial Crops and Products* 176, article 114364. DOI: 10.1016/j.indcrop.2021.114364

Wang, L.-Y., Wei, Y., Deng, H.-B., Lyu, R.-Q., Zhu, J.-J., and Yang, Y.-B. (2021). "Synergistic flame retardant effect of barium phytate and intumescent flame retardant for epoxy resin," *Polymers* 17, 2900-2900. DOI: 10.3390/polym13172900

Wang, R., Li, Y., Wang, Y., and Fang, Z. (2020). "Phosphorus-doped graphite felt allowing stabilized electrochemical interface and hierarchical pore structure for redox flow battery," *Applied Energy* 261, article 114369. DOI: 10.1002/chem.201802040

Xia, Y., Jin, F., Mao, Z., Guan, Y., and Zheng, A. (2014). "Effects of ammonium polyphosphate to pentaery-thritol ratio on composition and properties of

---

carbonaceous foam deriving from intumescent flame-retardant polypropylene,” *Polymer Degradation and Stability* 107, 64-73. DOI: 10.1016/j.polymdegradstab.2014.04.016

Xiong, P.-Q., Zhang, Y., Du, X.-Y., Song, P.-G., and Fang, Z.-P. (2019). “Green and scalable fabrication of core-shell biobased flame retardants for reducing flammability of polylactic acid,” *ACS Sustainable Chemistry Engineering* 7(9), 8954-8963. DOI: 10.1021/acssuschemeng.9b01016

Yang, C., Liang, G., Gu, A., and Yuan, L. (2013). “Flame retardancy and mechanism of bismaleimide resins based on a unique inorganic–organic hybridized intumescent flame retardant,” *Ind. Eng. Chem. Res.* 52, 15075-15087. DOI: 10.1021/ie402047v

Yang, S., Zhang, Q., and Hu, Y. (2016). “Synthesis of a novel flame retardant containing phosphorus, nitrogen and boron and its application in flame-retardant epoxy resin,” *Polymer Degradation and Stability* 133, 358-366. DOI: 10.1016/j.polymdegradstab.2016.09.023

Yuan, B., Xing, W., Hu, Y., Mu, X., Wang, J., Tai, Q., Li, G., Liu, L., Liew, K. M., and Hu, Y. (2016). “Boron/phosphorus doping for retarding the oxidation of reduced graphene oxide,” *Carbon* 101, 152-158. DOI: 10.1016/j.carbon.2016.01.080

Yu, H., Xia, Y., Xu, X., Zarshad, N., Wu, M., and Ni, H. (2020). “Preparation of organic-inorganic intumescent flame retardant with phosphorus, nitrogen and silicon and its flame retardant effect for epoxy resin,” *Journal of Applied Polymer Science* 137(41), article 49256. DOI: 10.1002/app.49256

Yu, Y., Ren, Z.-Y., Shang, Q.-Q., Hann, J.-G., Li, L., Chen, J.-Q., Fakudze, S., Tian, Z.-Q., and Liu, C.-G. (2021). “Ionic liquid-induced low temperature graphitization of cellulose-derived biochar for high performance sodium storage,” *Surface and Coatings Technology* 412, article 127034. DOI: 10.1016/j.surfcoat.2021.127034

Zhang, D., Lu, L.-G., Chen, L., and Wang, Y.-Q. (2022). “Synthesis of novel calixarene-based intumescent flame retardant and application of flame retardant epoxy resin,” *Journal of Applied Polymer Science* 139(16), article 51986. DOI: 10.1002/app.51986

Zhang, L.-L., Xu, J.-S., Shen, H.-Y., Xu, J.-Q., and Cao, J.-Z. (2021). “Montmorillonite-catalyzed furfurylated wood for flame retardancy,” *Fire Safety Journal* 121. DOI: 10.1016/j.firesaf.2021.103297

Zhang, X., Zhang, W., Zeng, G., Du, J., Zhang, W., and Yang, R. (2020). “The effect of different smoke suppressants with APP for enhancing the flame retardancy and smoke suppression on vinyl ester resin,” *Polymer Engineering and Science* 60, 314-322. DOI: 10.1002/pen.25286

Zheng, X. T., Dong, Y. Q., Liu, X. D., Xu, Y. L., and Jian, R. K. (2022). “Fully bio-based flame-retardant cotton fabrics via layer-by-layer self assembly of laccase and phytic acid,” *J. Cleaner Prod.* 350, article 131525. DOI: 10.1016/j.jclepro.2022.131525

Zhu, S., Gong, W., Luo, J., Meng, X., Xin, Z., Wu, J., and Jiang, Z. (2019). “Flame retardancy and mechanism of novel phosphorus-silicon flame retardant based on polysilsesquioxane,” *Polymers* 11(8), article 1304. DOI: 10.3390/polym11081304